The 1997–98 El Niño Evolution Relative to Previous El Niño Events

CHUNZAI WANG AND ROBERT H. WEISBERG

Department of Marine Science, University of South Florida, St. Petersburg, Florida

(Manuscript received 21 May 1998, in final form 19 March 1999)

ABSTRACT

The evolution of the 1997–98 El Niño is described using NCEP SST and OLR data, NCEP–NCAR reanalysis sea level pressure (SLP) fields, and The Florida State University surface wind data. From November 1996 to January 1997, the eastern Pacific is characterized by equatorial cold SST and high SLP anomalies, while the western Pacific is marked by off-equatorial warm SST anomalies and off-equatorial anomalous cyclones. Corresponding to this distribution are high OLR anomalies in the equatorial central Pacific and low OLR anomalies in the off-equatorial far western Pacific. The off-equatorial anomalous cyclones in the western Pacific are associated with a switch in the equatorial wind anomalies over the western Pacific from easterly to westerly. These equatorial westerly anomalies then appear to initiate early SST warmings around the date line in January/February 1997 and around the far eastern Pacific in March 1997. Subsequently, both the westerly wind and warm SST anomalies, along with the low OLR anomalies, grow and progress eastward. The eastward propagating warm SST anomalies merge with the slower westward spreading warm SST anomalies from the far eastern Pacific to form large-scale warming in the equatorial eastern and central Pacific. The anomaly patterns in the eastern and central Pacific continue to develop, reaching their peak values around December 1997. In the western Pacific, the off-equatorial SST anomalies reverse sign from warm to cold. Correspondingly, the off-equatorial SLP anomalies in the western Pacific also switch sign from low to high. These off-equatorial high SLP anomalies initiate equatorial easterly wind anomalies over the far western Pacific. Like the equatorial westerly wind anomalies that initiate the early warming, the equatorial easterly wind anomalies over the far western Pacific appear to have a cooling effect in the east and hence help facilitate the 1997–98 El Niño decay. This paper also compares the 1997–98 El Niño with previous warm events and discusses different ENSO mechanisms relevant to the 1997–98 El Niño.

1. Introduction

The term El Niño was originally used to denote the annual occurrence of a warm ocean current that flowed southward along the west coast of Peru and Ecuador around Christmastime. Subsequently, this term became associated with unusually strong warmings that occur interannually in relation with basin-scale tropical Pacific Ocean anomalies and global changes in climate patterns. The atmospheric counterpart to El Niño is termed the Southern Oscillation measured by an interannual seesaw in the tropical sea level pressure (SLP) between the western and eastern hemispheres. During El Niño, an unusually high SLP develops in the western tropical Pacific and an unusually low SLP develops in the southeastern tropical Pacific. The combined oceanic and atmospheric phenomenon is known as the El Niño–Southern Oscillation (ENSO). The opposite of El Niño is termed La Niña.

This interannual climate phenomenon was attributed to interactions between the tropical Pacific Ocean and atmosphere (Bjerknes 1969) and has been extensively studied over the past decades (e.g., Philander 1990; McCreary and Anderson 1991; Neelin et al. 1998). In the tropical Pacific, the westward blowing trade winds normally cause warm surface water to accumulate west of the date line forming the western Pacific warm pool. Associated with this western Pacific warm pool is intensive atmospheric convection, whereby air rises and flows aloft toward the eastern Pacific where it sinks to close the zonal circulation cell referred to as the Walker circulation. During El Niño, these patterns of sea surface temperature (SST) and atmospheric convection sidle eastward into the equatorial central Pacific, resulting in a weakening of the Walker circulation and the trade winds.

Thus, when an El Niño occurs, its signature is observed in both oceanic and atmospheric variables in different regions. Figure 1 shows the 3-month running means of SST anomalies in the Niño-3 region (5°S–5°N, 150°–90°W), zonal wind anomalies in the Niño-4 region (5°S–5°N, 160°E–150°W), outgoing longwave radiation (OLR) anomalies in the Niño-4 region, and the Southern Oscillation index (SOI) defined as the SLP anomaly

Corresponding author address: Dr. Chunzai Wang, Physical Oceanography Division, NOAA/Atlantic Oceanographic and Meteorological Laboratory, 4301 Rickenbacker Causeway, Miami, FL 33149.
E-mail: wang@aoml.noaa.gov

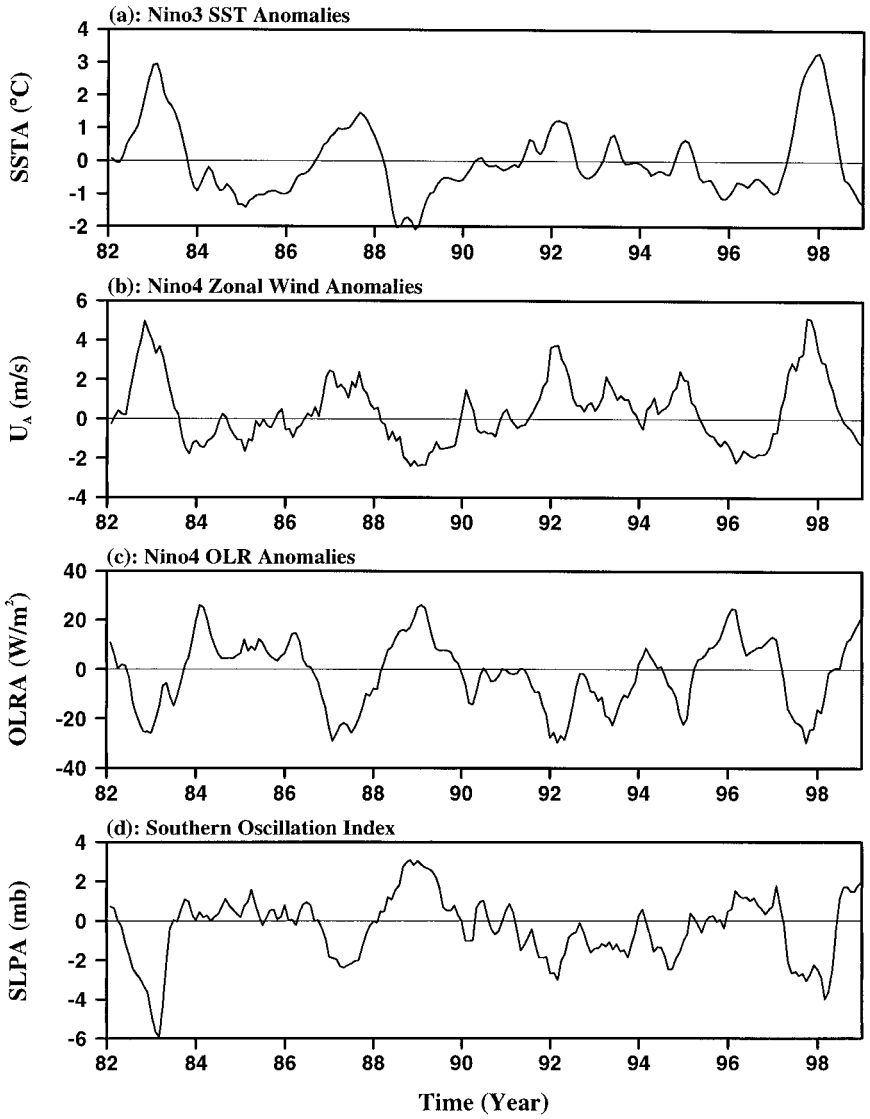

FIG. 1. The 3-month running means of (a) SST anomalies in the Niño-3 region (5°S–5°N, 150°–90°W), (b) zonal wind anomalies in the Niño-4 region (5°S–5°N, 160°E–150°W), (c) OLR anomalies in the Niño-4 region, and (d) SOI defined as SLP anomaly difference between Tahiti (17.5°S, 149.6°W) and Darwin (12.4°S, 130.9°E).

difference between Tahiti and Darwin. The warm (cold) SST anomalies in the equatorial eastern Pacific are accompanied by westerly (easterly) wind anomalies, low (high) OLR anomalies in the equatorial central Pacific, and a low (high) SOI. All of these indices show that 1997–98 is an El Niño year [also see Bell and Halpert (1998)]. The indices of Niño-3 SST and Niño-4 zonal wind anomalies show that the 1997–98 El Niño is the strongest event on record (the 1982–83 El Niño was previously considered the strongest event). The purpose of this paper is to describe the evolution of the 1997–98 El Niño using available oceanic and atmospheric data and model-derived reanalysis fields. The paper also compares the 1997–98 El Niño with previous warm events and discusses different ENSO mechanisms relevant to the 1997–98 El Niño.

2. Data

Monthly SST, SLP, OLR, and surface wind data are used in this study. SST data are taken from the National Centers for Environmental Prediction (NCEP) optimum interpolation (OI) global SST dataset on a 1° lat × 1° long grid. This OI SST product uses in situ (ship and buoy) SST data, satellite SST retrievals, and data on sea-ice coverage. A detailed description is given by Reynolds and Smith (1994, 1995) and Smith et al. (1996). SLP is from the NCEP–National Center for At-

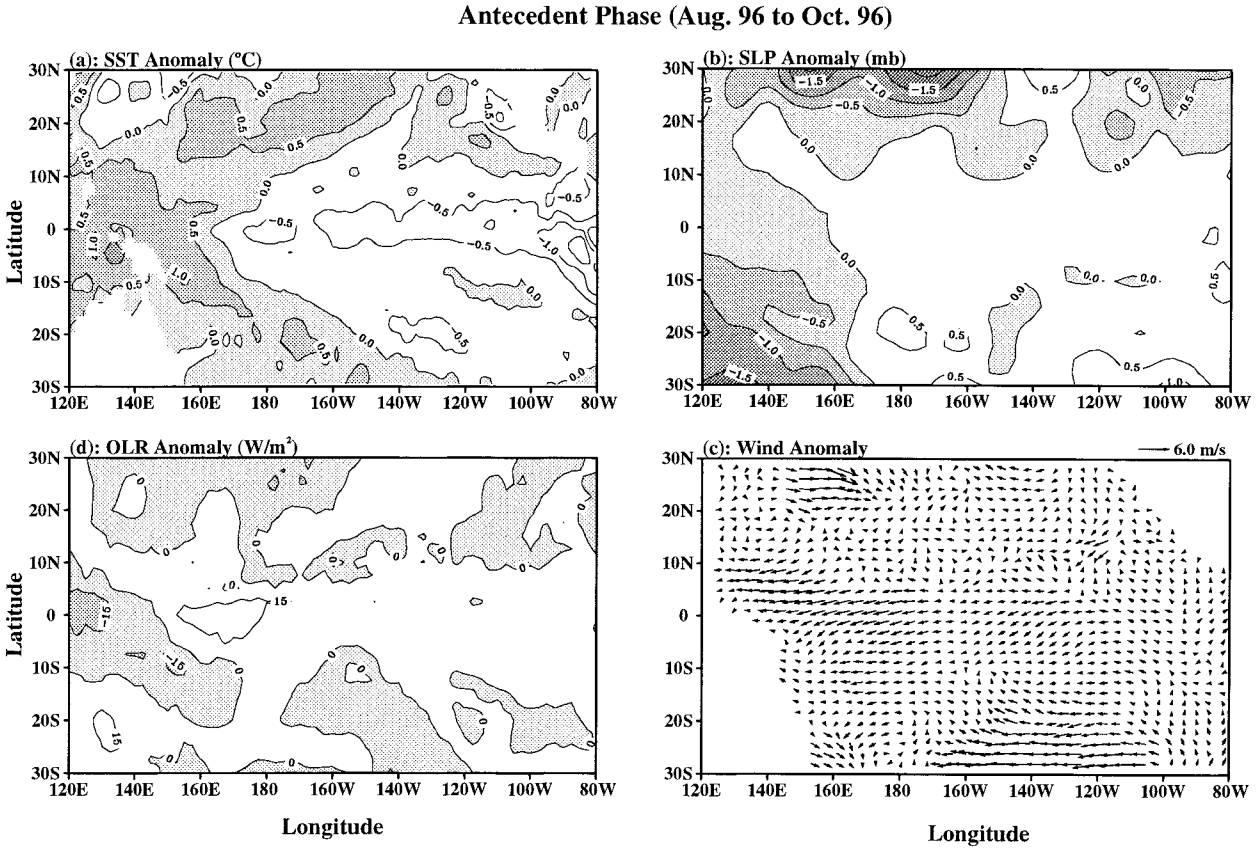

FIG. 2. The horizontal structures of the tropical Pacific (a) SST anomalies, (b) SLP anomalies, (c) wind anomalies, and (d) OLR anomalies in the antecedent phase (Aug 1996–Oct 1996) of the 1997–98 El Niño.

mospheric Research (NCAR) reanalysis fields on a 2.5° lat × 2.5° long grid. These model-derived reanalysis fields use a state-of-the-art global data assimilation system [see Kalnay et al. (1996) for details]. OLR data, on the grid of 2.5° lat × 2.5° long, are also taken from NCEP. OLR is controlled by the temperature of the emitting substance, so the cold cloud tops produce low OLR values and a relatively dry, cloudless atmosphere is associated with high OLR values. OLR is thus an indicator of atmospheric convective activity. Surface wind data are from The Florida State University (FSU) pseudo–wind stress on a 2° lat × 2° long grid. These pseudo–wind stress data were analyzed from ship and buoy wind data, including the Tropical Atmosphere Ocean (TAO) array winds [see Stricherz et al. (1997) for details]. The zonal and meridional wind velocity components (u and v) are calculated using zonal and meridional pseudo–wind stresses (W_x and W_y): $u = W_x/(W_x^2 + W_y^2)^{1/4}$, $v = W_y/(W_x^2 + W_y^2)^{1/4}$. For this study, analyses are focused on anomalies that are calculated by subtracting the monthly climatologies for each dataset from the data.

3. The 1997–98 El Niño

We first consider the pattern evolution for the 1997–98 El Niño over six phases: antecedent (Aug 1996–Oct 1996); onset (Nov 1996–Jan 1997); development (Mar 1997–May 1997); transition (Jul 1997–Sep 1997); mature (Nov 1997–Jan 1998); and decay (Feb 1998–Apr 1998). Rasmusson and Carpenter (1982) defined the first five phases and considered the time span from March to May of the El Niño year to be the ''peak phase'' because the South American coast reached its peak warming during that period for the El Niño events between 1949 and 1976. In view of the fact that the coastal warmings for the El Niño events between 1977 and 1992 occur in the boreal spring subsequent to the El Niño year rather than in the boreal spring of the El Niño year, Wang (1995) changed the peak phase to the development phase. For this study, the terminology of Wang (1995) is used since March to May of the El Niño year is a development stage of El Niño based on the different ENSO indices shown in Fig. 1. The decay phase is also added for examining the termination of the 1997–98 El Niño. With these definitions, the horizontal patterns for six different stages of the 1997–98 El Niño are shown in Figs. 2–7 for averages of properties over these time periods.

The antecedent phase (Fig. 2) exhibits La Niña conditions. Observed are cold SST anomalies in the equatorial eastern and central Pacific, and warm SST anom-

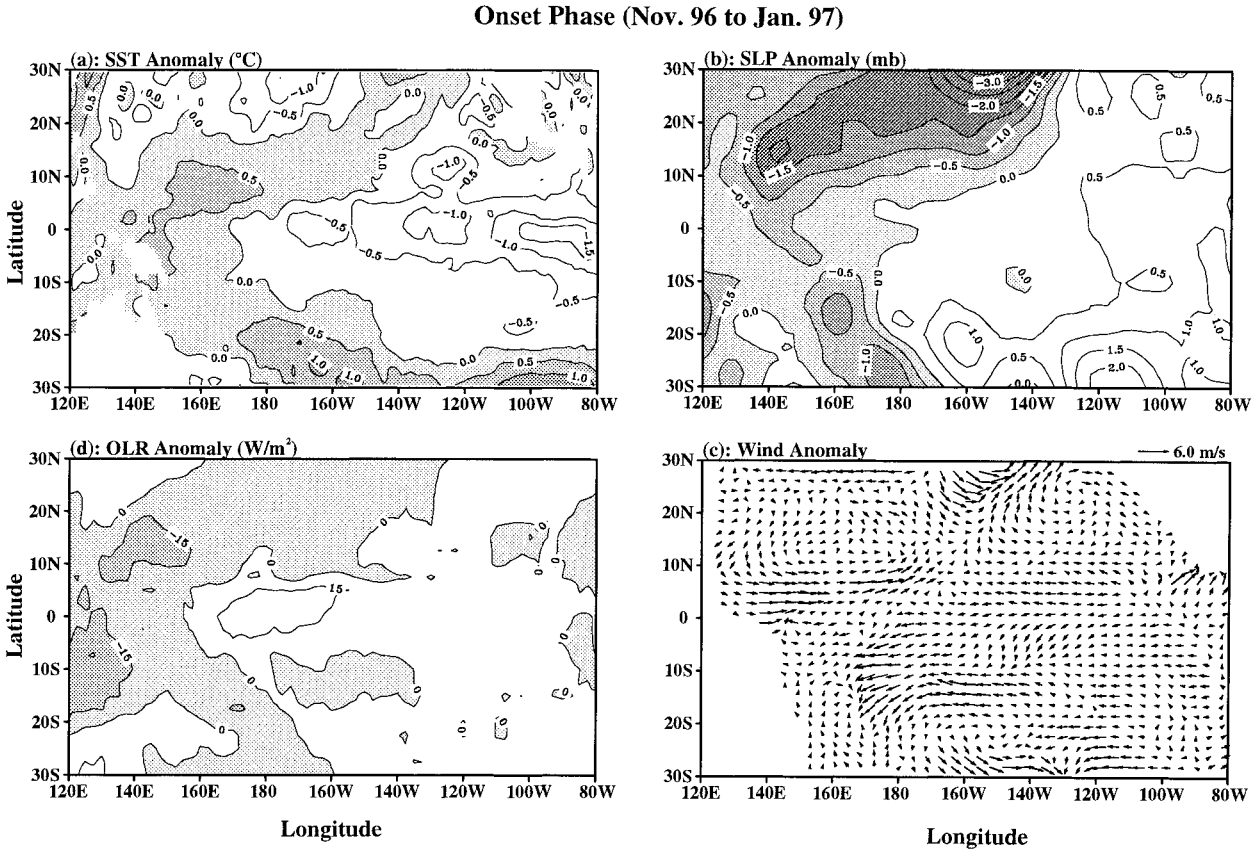

FIG. 3. The horizontal structures of the tropical Pacific (a) SST anomalies, (b) SLP anomalies, (c) wind anomalies, and (d) OLR anomalies in the onset phase (Nov 1996–Jan 1997) of the 1997–98 El Niño.

alies in the tropical western Pacific. SLP anomalies are nearly normal in the tropical eastern and central Pacific, whereas they are low over the western Pacific. Two midlatitude subtropical anomalous cyclones exist: one in the Southern Hemisphere (SH) over Australia, and the other in the Northern Hemisphere (NH) between 140°E and 160°W. Associated with the equatorial distributions of SST and SLP anomalies, the equatorial Pacific displays anomalous easterly winds (Gill 1980), with the strongest wind anomalies in the equatorial western Pacific. Negative OLR anomalies are correspondingly located over the equatorial far western Pacific, whereas positive values are in the equatorial central and eastern Pacific. The distribution of OLR anomalies indicates that atmospheric convection occurs over the equatorial far western Pacific during that time.

During the onset phase (Fig. 3) cold SST anomalies remain over the equatorial eastern and central Pacific, while warm SST anomalies develop in the off-equatorial western Pacific with maximum values around 10°N and to the south of the normal position of the South Pacific convergence zone. Associated with these SST patterns are high SLP anomalies in the eastern Pacific and off-equatorial anomalous cyclones in the NH and SH over the western Pacific. These developing off-equatorial anomalous cyclones appear as tropical extensions of the subtropical anomalous cyclones observed in the antecedent phase, and they form over the off-equatorial warm SST anomalies. Note that SLP climatologies during that time are low SLP in the Tropics and high SLP in the subtropics, and a decrease in western Pacific tropical and subtropical total SLP fields is associated with appearance of the off-equatorial anomalous cyclones (not shown). As a result of the off-equatorial anomalous cyclone pair (the NH cyclone is stronger during the onset phase of the 1997–98 El Niño), equatorial easterly wind anomalies in the western Pacific reverse to westerly. These equatorial westerly anomalies in the western Pacific herald the development of the 1997–98 El Niño since they induce eastward propagating downwelling Kelvin waves in the leading phase of Kelvin waves bringing subsequent warming to the central and eastern Pacific (e.g.,Wyrtki 1975; McCreary 1976; Busalacchi and O'Brien 1981; Philander 1981). The downwelling Kelvin wave–induced warming in the east by equatorial westerly wind anomalies is evidenced in sea surface height field from the TOPEX/Poseidon altimeter and thermocline depth from the TAO array (e.g., Yu and Rienecker 1998; McPhaden 1999). Associated with the western Pacific SST and SLP anomalies, OLR anom-

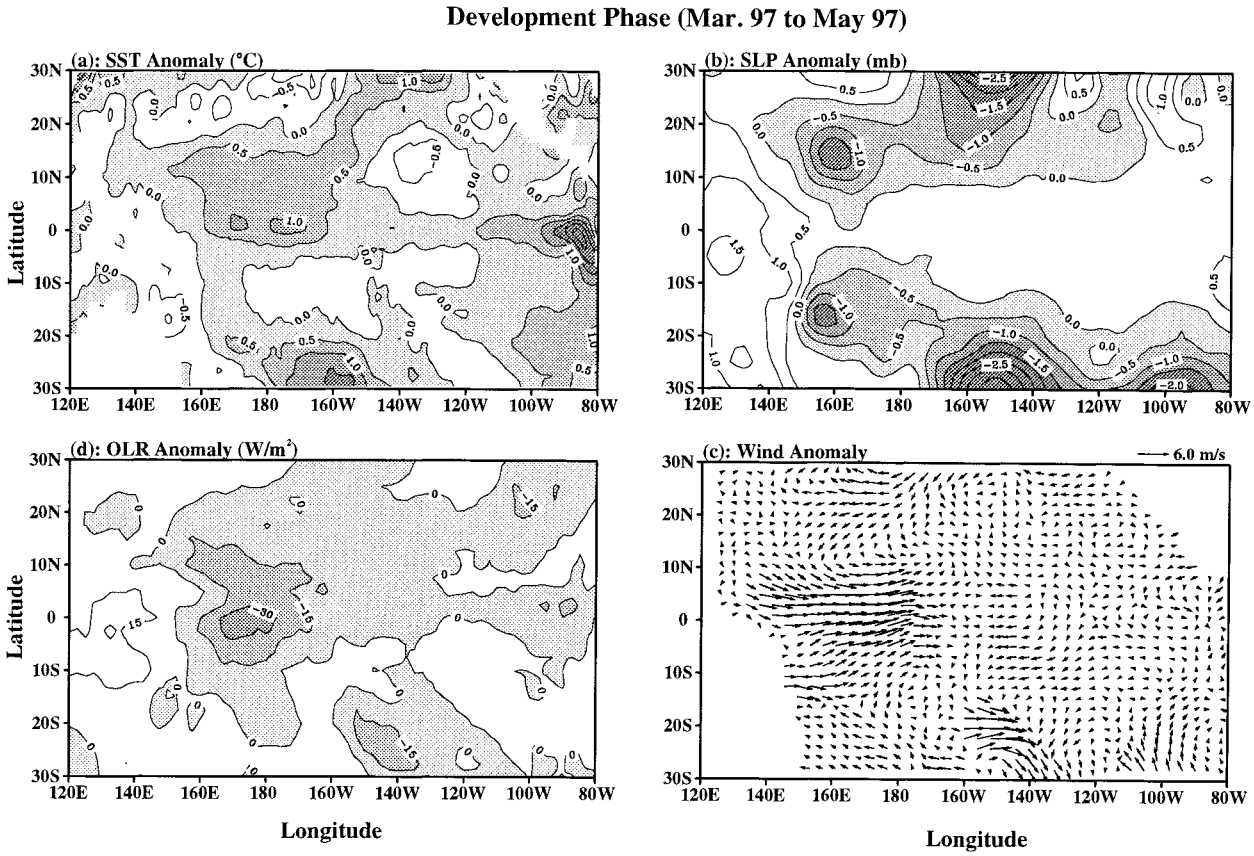

FIG. 4. The horizontal structures of the tropical Pacific (a) SST anomalies, (b) SLP anomalies, (c) wind anomalies, and (d) OLR anomalies in the development phase (Mar 1997–May 1997) of the 1997–98 El Niño.

alies also show an off-equatorial western Pacific pattern with the lowest anomalies located about 10°N and S in the far western Pacific.

The 1997–98 El Niño begins to develop after the reversal of the wind anomalies in the equatorial western Pacific (Fig. 4). Equatorial warmings occur both around the date line and in the far eastern Pacific, with large warm SST anomalies in the far eastern Pacific. SLP shows a well-organized, symmetric, off-equatorial low anomaly pattern in the western Pacific with correspondingly anomalous cyclonic flows in the NH and the SH (the twin anomalous cyclones are located around 15°N, 158°E and 15°S, 158°E, respectively). Therefore, the equatorial westerly wind anomalies in the western Pacific are further developed in both magnitude and fetch, and easterly wind anomalies occur around 25°N and S in the western Pacific. Associated with these developments is the eastward movement of the equatorial low OLR anomalies toward the date line, indicating that the Walker circulation has shifted eastward. The eastward shift of the Walker circulation associated with atmospheric deep convection (low OLR values) in turn favors westerly wind anomaly growth and hence further warming in the east.

Following the development of equatorial westerly wind anomalies in the western Pacific, the transition phase (Fig. 5) shows a large-scale warming in the equatorial eastern and central Pacific. SST anomalies in the off-equatorial western Pacific have now switched sign from warm to cold. This SST anomaly sign switch in the off-equatorial western Pacific may be due to off-equatorial wind curl–induced Ekman pumping (SLP determines wind patterns and hence wind curl that in turn alters SST through Ekman pumping). Correspondingly, the off-equatorial western Pacific SLP anomalies undergo transition with the low SLP anomalies in the SH reversing to high SLP anomalies due to the relatively large area of cold SST anomalies there (Gill 1980). SLP in the eastern Pacific shows low SLP anomalies. The equatorial westerly winds continue their development and now penetrate eastward to 120°W. Near the normal position of the intertropical convergence zone (ITCZ) between 170° and 130°W, northerly wind anomalies appear and northeasterly wind anomalies occur east of 130°W, perhaps due to a southward shift of the ITCZ toward the equatorial region of anomalous warming. The southeast Pacific shows strong westerly wind anomalies, consistent with low SLP anomalies there. Associated with SST and SLP anomalies, low OLR anomalies now cover the entire equatorial central and eastern

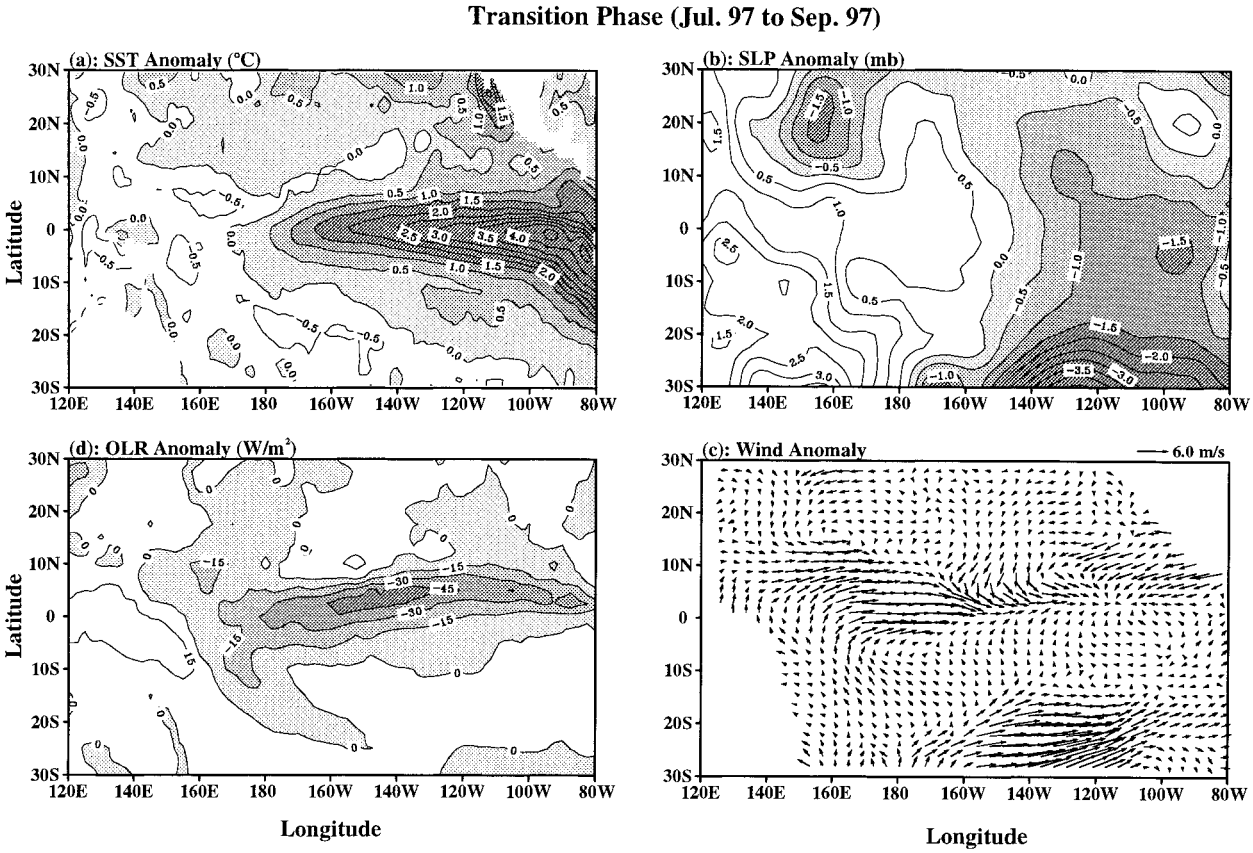

FIG. 5. The horizontal structures of the tropical Pacific (a) SST anomalies, (b) SLP anomalies, (c) wind anomalies, and (d) OLR anomalies in the transition phase (Jul 1997–Sep 1997) of the 1997–98 El Niño.

Pacific. The OLR anomaly distribution suggests that atmospheric deep convection associated with the Walker circulation has been further shifted eastward during that time.

In the mature phase (Fig. 6), the equatorial eastern Pacific shows maximum anomalous warming, whereas the off-equatorial western–central Pacific shows cold SST anomalies. Similar to that in the SH during the transition phase, the SLP anomalies in the NH have now also reversed sign to become high SLP anomalies. Corresponding with these patterns of off-equatorial high SLP in the western Pacific, equatorial easterly wind anomalies are initiated over the far western Pacific. These equatorial easterly wind anomalies force eastward propagating upwelling Kelvin waves that help terminate El Niño (e.g., Tang and Weisberg 1984; Philander 1985). Northerly wind anomalies occur north of the equator in the central and eastern Pacific, reflecting the southward movement of the ITCZ. Associated with this enhanced seasonal migration of the ITCZ the region of maximum westerly wind anomalies in the central Pacific is pushed to the south of the equator. During the mature phase, equatorial central Pacific low OLR anomalies are now fully developed, whereas the western Pacific appears to be convection free with maximum high OLR anomalies located in the far western Pacific near 12°N.

With the initiation of equatorial easterly wind anomalies over the western Pacific, warm SST anomalies in the equatorial eastern Pacific begin to decay, whereas the cold SST anomalies in the off-equatorial western–central Pacific continue to develop (Fig. 7). Associated with the off-equatorial cold SST anomaly regions, high SLP anomalies develop further resulting in an increase in the equatorial easterly wind anomalies over the western Pacific. This causes a further relaxation in the warm SST anomalies in the equatorial eastern Pacific. During this decay phase, northerly wind anomalies to the north of the equator in the central and eastern Pacific continue to blow, and the region of maximum westerly wind anomalies in the central Pacific is further pushed to the south of the equator. This SH translation of the westerly wind anomaly patterns also facilitates the 1997–98 El Niño decay since it causes a relaxation of westerly anomalies on the equator. In the decay phase, low OLR anomalies continue to cover the entire equatorial central and eastern Pacific; however, a transition appears to be developing in the far western Pacific as warm SST anomalies again begin to take root.

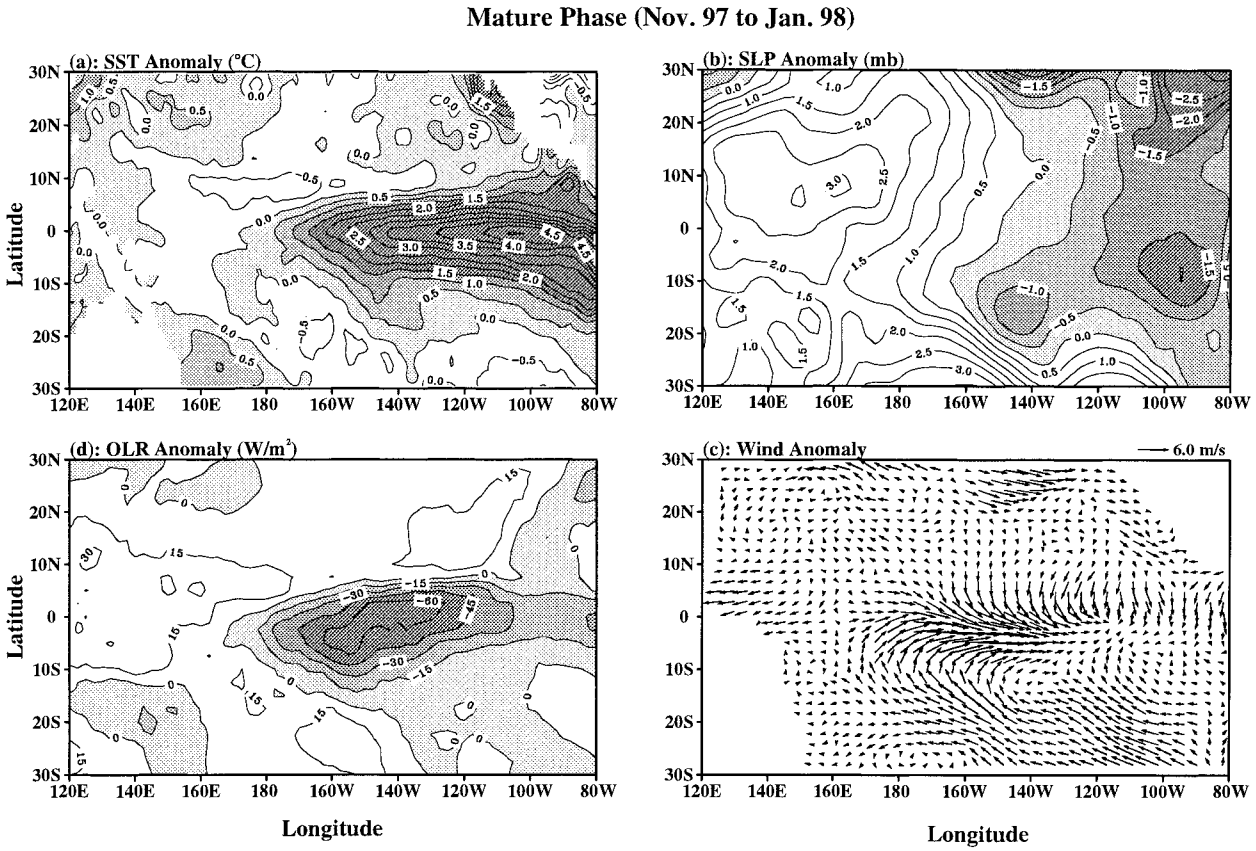

FIG. 6. The horizontal structures of the tropical Pacific (a) SST anomalies, (b) SLP anomalies, (c) wind anomalies, and (d) OLR anomalies in the mature phase (Nov 1997–Jan 1998) of the 1997–98 El Niño.

How the 1997–98 El Niño develops and decays can be further demonstrated by time–longitude plots of SST, SLP, zonal wind, and OLR anomalies along the equator, as shown in Fig. 8. Equatorial westerly wind anomalies appear over the far western Pacific in November/December 1996. The continuous westerly anomalies and their eastward penetration are associated with an initial warming in January/February 1997 in the equatorial central Pacific. The warming also appears in March 1997 along the South American coast. The warm SST anomalies in the equatorial central Pacific propagate eastward, whereas the warm SST anomalies in the far eastern Pacific grow and spread westward. In June 1997, the eastward propagating and westward spreading SST anomalies merge together, forming a large-scale warming in the equatorial central and eastern Pacific. Then, the warm SST anomalies grow but do not propagate. Note that the eastward propagating SST anomalies may be attributed to Kelvin waves, whereas the westward spreading SST anomalies may be due to Rossby waves reflected at the eastern boundary. OLR and zonal wind anomalies also propagate eastward, whereas the SLP anomalies seem to change synchronously. Figures 1 and 8 show that the zonal wind anomalies lead the SST anomalies, suggesting that atmospheric wind and SLP patterns (SLP determines wind) are precursors for the development and decay of the 1997–98 El Niño. In particular, both the equatorial westerly and easterly wind anomalies that are initiated over the far western Pacific by off-equatorial SLP anomalies lead the initial warmings and the decay phase of the 1997–98 El Niño, respectively. This relationship is consistent with earlier studies by Wyrtki (1975), McCreary (1976), Busalacchi and O'Brien (1981), and Philander (1981) who showed that westerly wind anomalies west of the date line produce evolving Kelvin waves of downwelling tendency that facilitate El Niño condition growth, and by Tang and Weisberg (1984) and Philander (1985) who demonstrated that easterly wind anomalies west of the date line force evolving Kelvin waves of opposite tendency that facilitate El Niño condition decay.

4. Comparison with previous El Niño events

Rasmusson and Carpenter (1982) provided a description of a composite El Niño scenario based on warm events that occured between 1949 and 1976. They showed that in the far eastern Pacific, El Niño begins around Christmastime and peaks in the boreal late spring of the El Niño year. On the other hand, in the Niño-3

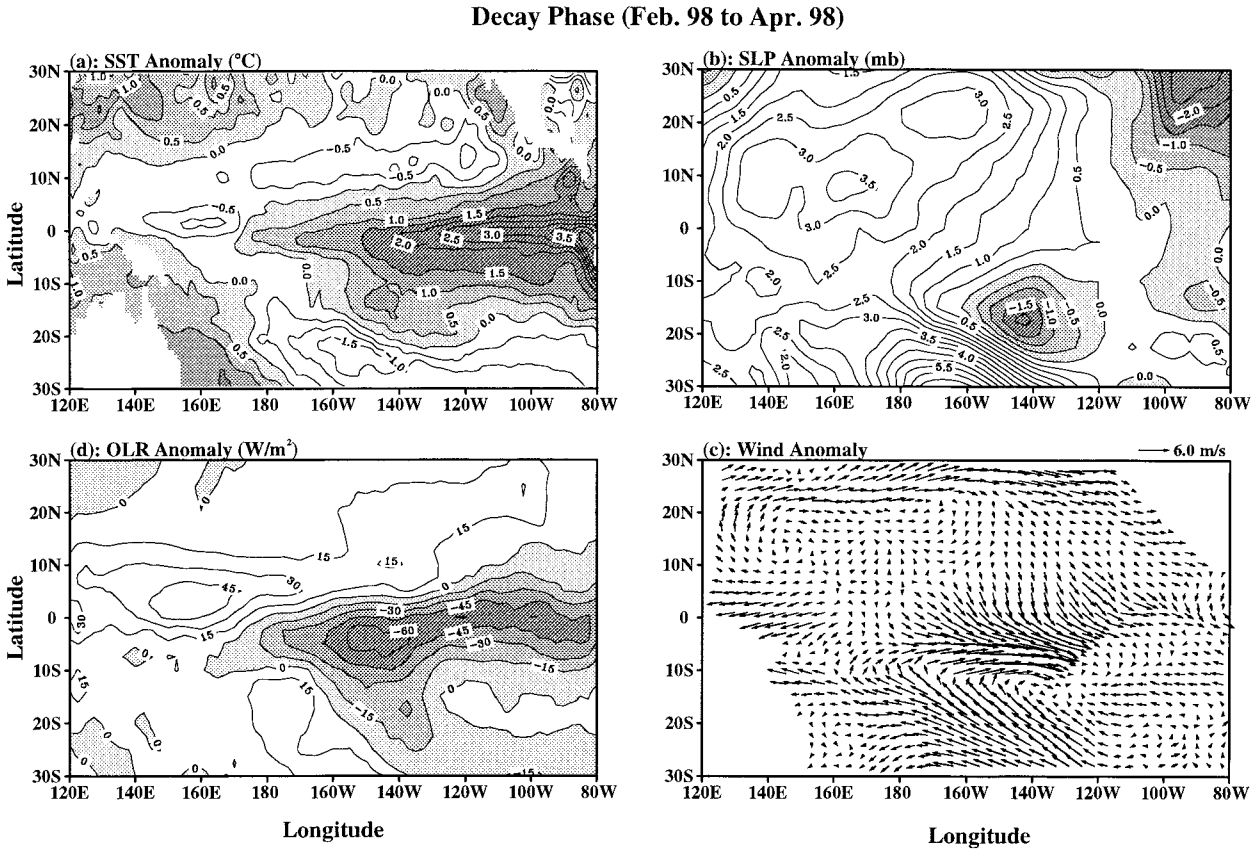

FIG. 7. The horizontal structures of the tropical Pacific (a) SST anomalies, (b) SLP anomalies, (c) wind anomalies, and (d) OLR anomalies in the decay phase (Feb 1998–Apr 1998) of the 1997–98 El Niño.

region positive SST anomalies occur in the boreal early spring and peak near the end of the El Niño year. In a comparative study of warm events over the past four decades, Wang (1995) showed that in the far eastern Pacific, there is a phase shift in the El Niño peak for events that occured after 1976. The far eastern Pacific peak phase for the El Niño events between 1977 and 1992 occurs in the boreal late spring subsequent to the El Niño year rather than the boreal late spring of the El Niño year (Wang 1995, see his Fig. 3). Are the peak phases of the 1997–98 El Niño different from previous El Niño events? Figure 9 shows the 3-month running mean SST anomalies from 1996 to 1998 in the regions of Niño-2 (0°–5°S, 90°–80°W), Niño-3, and Niño-3.4 (5°N–5°S, 170°–120°W). In all of these regions, the SST anomalies become positive in early spring 1997 and the peak phase occurs in December 1997. The warm SST anomalies are the highest in the far eastern Pacific and decrease toward the west. The Niño-2 SST anomalies show a second peak in the sping 1998. Therefore, peak phase of all El Niño events from 1949 to 1999 in the eastern and central Pacific is near the end of the El Niño year. The far eastern Pacific peak phase for the 1997–98 El Niño shows double peaks with one around the end of 1997 and the other around the spring of 1998. This is different from the far eastern Pacific peak phases for the El Niño events from 1949 to 1976 and for the El Niño events from 1977 to 1992 that occurred in the boreal spring of the El Niño year and in the boreal late spring subsequent to the El Niño year, respectively.

In a study of ENSO western Pacific variability, Wang et al. (1999) obtained composite horizontal structure patterns for peak El Niño and La Niña using the Comprehensive Ocean–Atmosphere Data Set (COADS; Woodruff et al. 1987) from January 1950 to December 1992 and OLR data from January 1974 to December 1992. The peak El Niño composite, shown in Fig. 10, was calculated by taking the average December anomaly of the El Niño years from 1950 to 1992. For this peak of El Niño composite, when maximum warm SST anomalies occur in the equatorial eastern Pacific, maximum cold SST anomalies are located to the north and south of the equator in the western Pacific rather than on the equator. Since the atmospheric convection over the western Pacific warm pool shifts to the equatorial central Pacific during the warm phase of ENSO, the region of low OLR anomalies is located to the west of equatorial eastern Pacific maximum warm SST anomalies. Similar to the relative position of the SST and OLR anomalies in the equatorial eastern and central Pacific, the off-

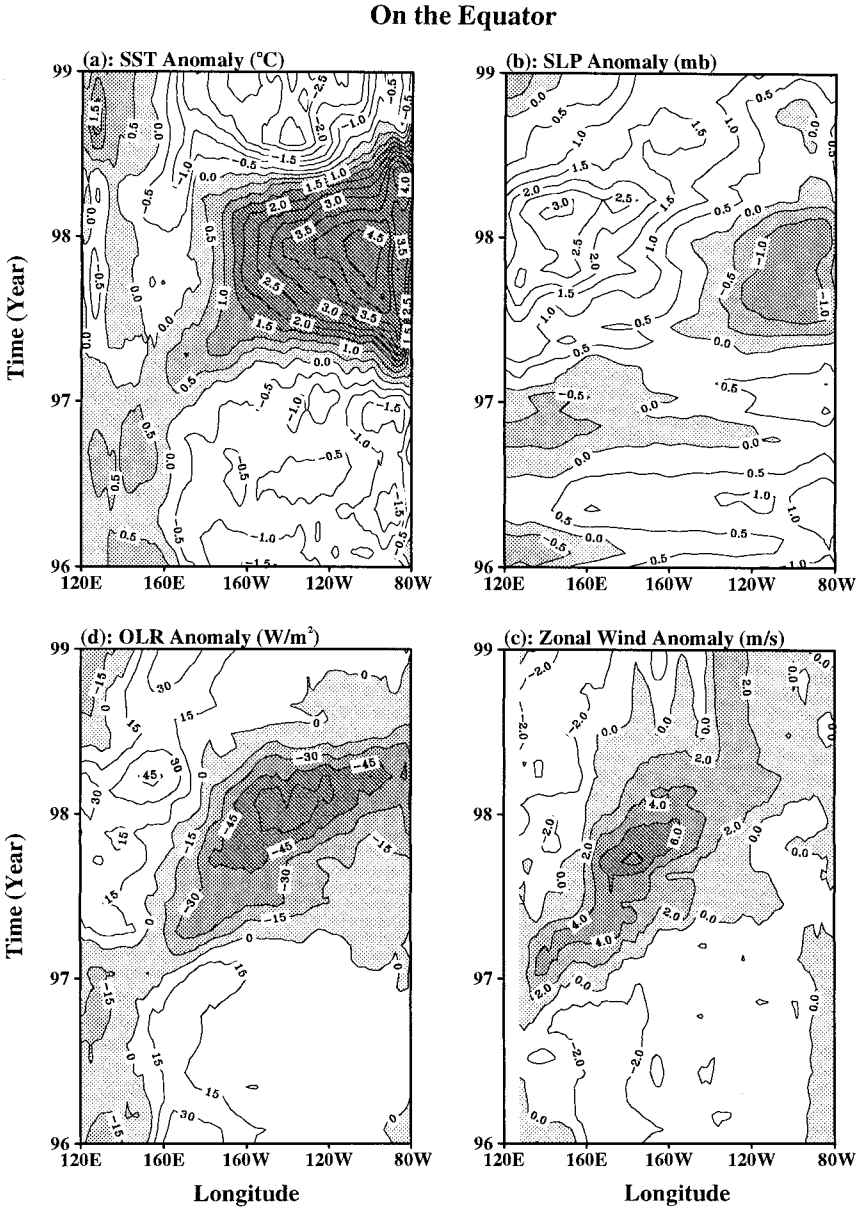

FIG. 8. The evolutions of 3-month running mean (a) SST anomalies, (b) SLP anomalies, (c) zonal wind anomalies, and (d) OLR anomalies along the equator from Jan 1996 to Dec 1998.

equatorial region of high OLR anomalies is positioned west of the off-equatorial region of cold SST anomalies in the western Pacific. The off-equatorial western Pacific cold SST anomalies are also accompanied by off-equatorial western Pacific high SLP anomalies. As shown in Fig. 10, the off-equatorial high SLP anomalies generate equatorially convergent wind anomalies that turn anticyclonically to equatorial easterly wind anomalies over the far western Pacific. The converse occurs during the cold phase of ENSO. The SST and wind composites of Rasmusson and Carpenter (1982) also showed off-equatorial western Pacific cold SST anomalies and equatorial easterly wind anomalies over the far western Pacific during the mature phase of ENSO (see their Fig. 21), although with smaller off-equatorial western Pacific SST anomaly magnitudes. As discussed in Wang et al. (1999), the magnitude differences may be the result of two factors: 1) the composite in Fig. 10 used the data from 1950 to 1992, whereas the composites of Rasmusson and Carpenter (1982) used the data from 1949 to 1976, and 2) the composites of Rasmusson and Carpenter (1982) used data that were filtered more in both time and space.

Comparing Figs. 6 and 10 shows that the basic features for the mature phase of the 1997–98 El Niño and for the peak El Niño composite between 1950 and 1992

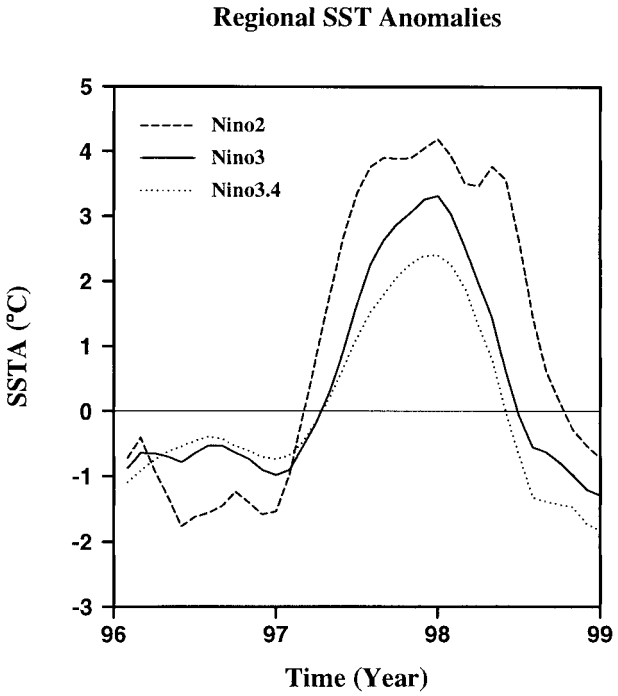

FIG. 9. The 3-month running means of SST anomalies in the Niño-2 (0°–5°S, 90°–80°W), Niño-3, and Niño-3.4 (5°N–5°S, 170°–120°W) regions from Jan 1996 to Dec 1998.

are similar although details are different. From November 1997 to January 1998, the off-equatorial western Pacific has cold SST and high SLP anomalies, and the off-equatorial far western Pacific has high OLR anomalies. At the same time, the equatorial eastern Pacific has warm SST and low SLP anomalies, and the equatorial central Pacific has low OLR anomalies. Equatorial westerly wind anomalies in the central Pacific and equatorial easterly wind anomalies in the far western Pacific are associated with these SST, SLP, and OLR anomaly patterns. However, the relative positions of the maximum anomalies are different. Maximum anomalies for the 1997–98 El Niño are located farther east compared to the composite El Niño between 1950 and 1992.

To compare the western Pacific interannual variability with the conventional ENSO indices in the central and eastern Pacific, Wang et al. (1999) defined two additional regional indices termed Niño-5 (5°S–5°N, 120°–140°E) and Niño-6 (8°–16°N, 140°–160°E), consistent with the observations reported therein. The Niño-6 SST anomalies are nearly out of phase with the Niño-3 SST anomalies, and the Niño-5 zonal wind anomalies are also approximately out of phase with the Niño-4 zonal wind anomalies. Figure 11 compares these indices for the period from January 1996 to December 1998. The westerly wind anomalies in the Niño-5 region peak about six to eight months before those in the Niño-4 region. When the westerly wind anomalies peak in the Niño-4 region, those in the Niño-5 region are easterly and growing in magnitude. The continous growth of the Niño-5 easterly wind anomalies are accompanied with decay of the Niño-4 westerly wind anomalies. The Niño-3 SST anomalies are also out of phase with the Niño-6 SST anomalies. The cold Niño-6 SST anomalies are weaker however, since the coldest off-equatorial SST anomalies during the 1997–98 El Niño occured to the east of the Niño-6 region. This is shown in Fig. 11 for the region of 8°–16°N and 180°–160°W, where a more pronounced amplitude is evident. Figure 11 also shows that the Niño-5 westerly wind onset (zonal wind anomaly becoming positive) leads the Niño-3 warming onset and that the Niño-5 easterly wind onset (zonal wind anomaly becoming negative) leads the Niño-3 SST anomaly decay phase. This suggests the importance of the equatorial zonal wind anomalies over the far western Pacific in the development and decay of the 1997–98 El Niño.

Rasmusson and Carpenter (1982) showed that the antecedent phase of El Niño for the warm events between 1949 and 1976 had significant easterly wind anomalies in the equatorial western and central Pacific (their Fig. 17), whereas Wang (1995) showed that the wind anomalies are small or even westerly during the antecedent phase of El Niño for the warm events between 1977 and 1992 (his Fig. 7a). The 1997–98 El Niño is similar to the warm events between 1949 and 1976 in that strong easterly wind anomalies did occur in the equatorial western Pacific during the antecedent phase because of the 1995–96 La Niña. Between the antecedent and development phases, the southeast trade winds over the southeast Pacific weakened during the warm events between 1949 and 1976 (with westerly wind anomalies) but they strengthened during the warm events between 1977 and 1992 (with easterly wind anomalies) [see Figs. 4, 6, and 7 of Wang (1995)]. In comparison, the 1997–98 El Niño shows that the wind anomalies over the southeast Pacific were nearly zero (Figs. 2–4). This may explain why the peak phase over the South American coast does not occur in spring 1997 since the wind fields did not favor spring coastal warming.

The onset phase of the 1997–98 El Niño shows off-equatorial anomalous cyclones in the western Pacific, with the NH cyclone being stronger (Fig. 3). During the development phase of the 1997–98 El Niño, the off-equatorial cyclones develop into twin cyclones (Fig. 4). These off-equatorial cyclones initiate equatorial westerly wind anomalies in the western Pacific that are responsible for the 1997–98 El Niño. Figure 12 shows the SLP and wind anomalies during the onset and development phases of the 1982–83 El Niño. The onset phase of the 1982–83 El Niño shows symmetric, off-equatorial anomalous cyclones that initiate equatorial westerly wind anomalies over the far western Pacific. During the development phase of the 1982–83 El Niño, it seems that equatorial westerly wind anomalies in the western Pacific are mainly controlled by the NH low SLP anomalies. Thus, the details for initiating westerly wind anomalies between the 1982–83 and 1997–98 El Niños

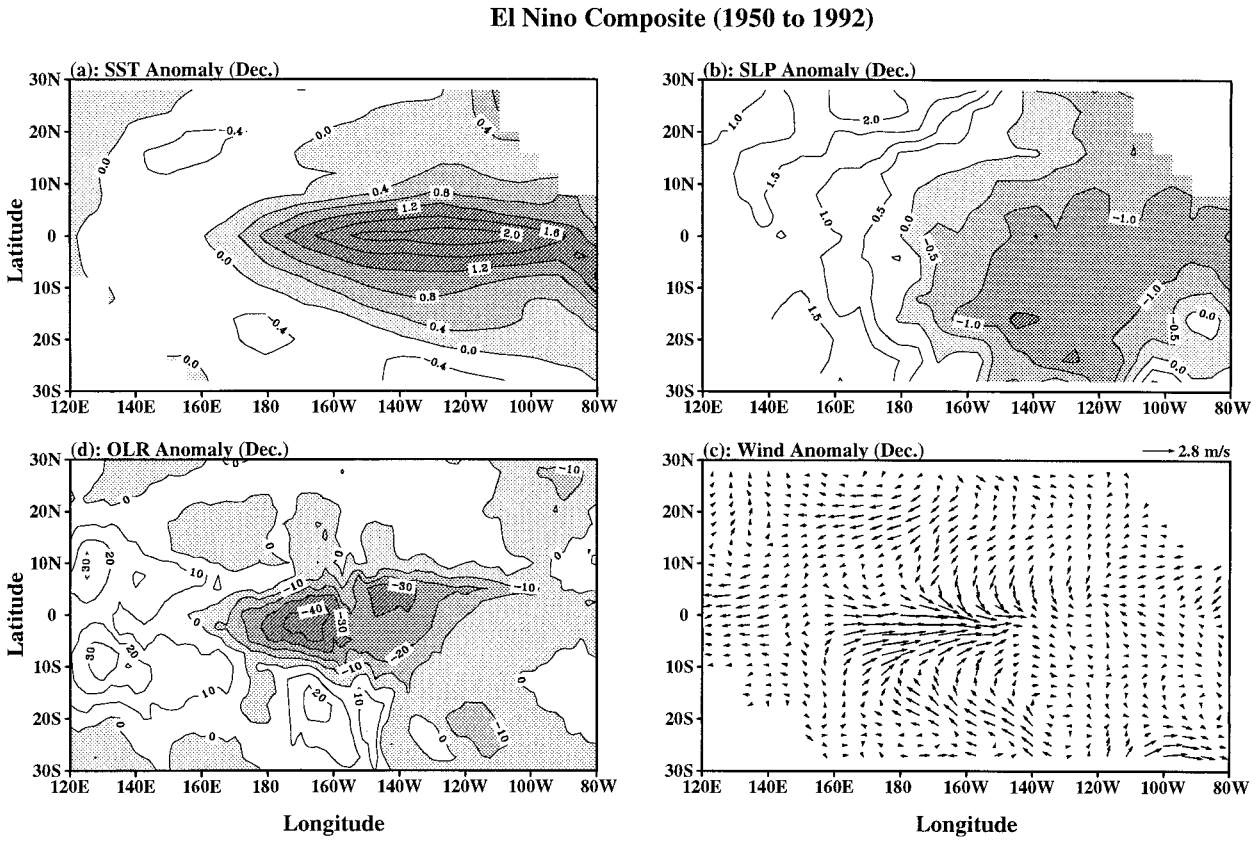

FIG. 10. The peak El Niño composite of (a) SST anomalies (°C), (b) SLP anomalies (mb), (c) surface wind anomalies (m s^{-1}), and (d) OLR anomalies (W m^{-2}). The composite is formed by taking the average Dec anomaly for 1957, 1965, 1972, 1982, 1986, and 1991 (Wang et al. 1999).

may be different. However, both of these warm events show the importance of equatorial westerly wind anomalies in the western Pacific and that these wind anomalies are initiated by off-equatorial low SLP anomaly patterns.

Finally, it is noted that meridional wind anomalies along with the ITCZ from the transition to decay phases vary between events. The transition phase of the warm events between 1949 and 1976 show strong northerly wind anomalies along the eastern Pacific ITCZ, whereas

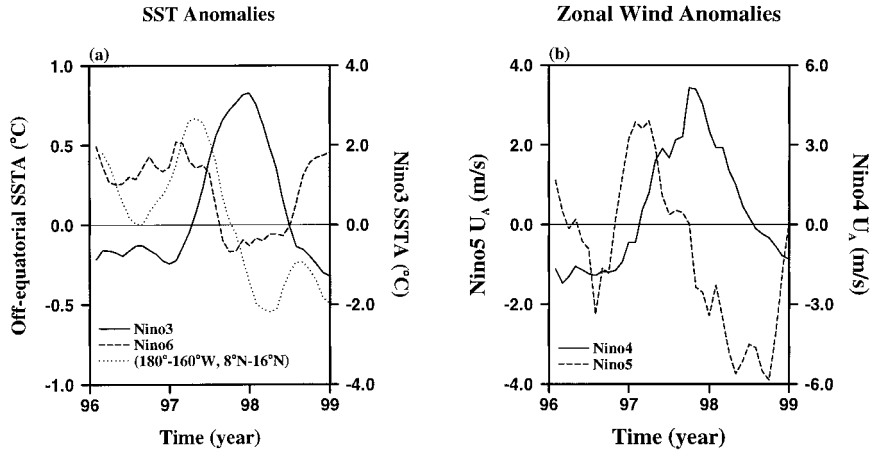

FIG. 11. The 3-month running means of (a) SST anomalies in the Niño-3 region, in the Niño-6 region (8°–16°N, 140°–160°E), and in the region of 8°–16°N, 180°–160°W, (b) zonal wind anomalies in the Niño-4 region and in the Niño-5 region (5°S–5°N, 120°–140°E).

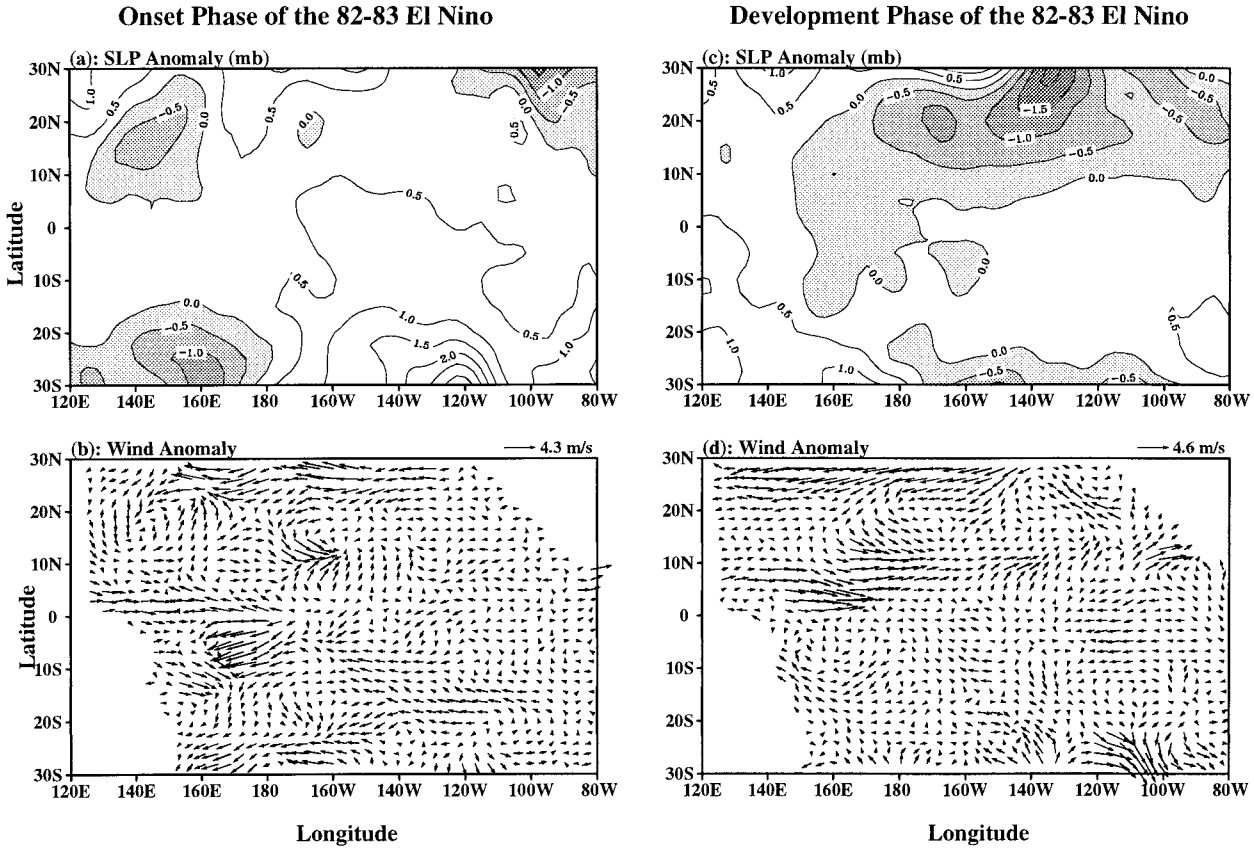

FIG. 12. The onset and development phases of the 1982–83 El Niño. (a) and (b) show SLP and wind anomalies in the onset phase of the 1982–83 El Niño (Nov 1981–Jan 1982). (c) and (d) show SLP and wind anomalies in the development phase of the 1982–83 El Niño (Mar 1982–May 1982).

the warm events between 1977 and 1992 are charaterized by weaker northerly wind anomalies [see Figs. 6d and 7d of Wang (1995)]. The 1997–98 El Niño is similar to the El Niño warm events between 1949 and 1976, showing strong northerly wind anomalies along the eastern Pacific ITCZ from the transition to decay phases (Figs. 5–7).

5. Summary and discussion

The oceanic and atmospheric data and model-derived reanalysis fields all suggest that the western Pacific is an important region for the evolution of the 1997–98 El Niño. The onset originates from the western Pacific from November 1996 to January 1997, when equatorial westerly wind anomalies over the western Pacific are initiated by off-equatorial anomalous cyclones. These western Pacific off-equatorial anomalous cyclones are associated with off-equatorial warm SST anomalies there and off-equatorial low OLR anomalies in the far western Pacific. The equatorial westerly wind anomalies over the western Pacific and their subsequent development induce eastward propagating downwelling Kelvin waves (e.g., Wyrtki 1975; McCreary 1976; Busalacchi and O'Brien 1981; Philander 1981) and associated ocean–atmosphere interaction feedbacks that cause warming in the east. Early equatorial warmings in the central Pacific and in the far eastern Pacific, therefore, occur around January/February 1997 and March 1997, respectively. Subsequently, equatorial warm SST anomalies in the central Pacific progress eastward due to eastward propagating Kelvin waves, and warm SST anomalies in the far eastern Pacific spread westward perhaps due to reflected Rossby waves at the eastern boundary. In June 1997, the eastward propagating and westward spreading SST anomalies merge together, forming a large-scale warming in the equatorial central and eastern Pacific. While warm SST anomalies in the equatorial central and eastern Pacific continue to grow, SST anomalies in the off-equatorial western Pacific reverse sign from warm to cold consistent with off-equatorial wind curl–induced Ekman pumping in the western Pacific. Correspondingly, off-equatorial SLP anomalies in the western Pacific undergo transition from low to high. The off-equatorial high SLP anomalies initiate equatorial easterly wind anomalies over the western Pacific between the transition and mature phases. These equatorial easterly wind anomalies over the western Pa-

cific and the subsequent development force eastward propagating upwelling Kelvin waves that help faciliate the 1997–98 El Niño decay (e.g., Tang and Weisberg 1984; Philander 1985). Thus, the western Pacific also plays a role in the termination of the 1997–98 El Niño.

How does the evolution of the 1997–98 El Niño fit previous different ENSO mechanisms? Three oscillator models have been reported to interpret ENSO: 1) the delayed oscillator (Suarez and Schopf 1988; Battisti and Hirst 1989; Cane et al. 1990), 2) the recharge–discharge oscillator Jin 1997), and 3) the western Pacific oscillator (Weisberg and Wang 1997a). Considering the effects of equatorially trapped oceanic waves propagating in a closed basin through a delay term, Suarez and Schopf (1988) and Battisti and Hirst (1989) introduced the delayed oscillator as a candidate mechanism for ENSO. It is represented by a single ordinary differential delay equation with positive and negative feedbacks. The positive feedback is represented by local ocean–atmosphere coupling in the equatorial eastern Pacific. The delayed negative feedback is represented by free Rossby waves generated in the eastern Pacific coupling region that propagate to and reflect from the western boundary, returning as Kelvin waves to reverse the anomaly pattern in the eastern Pacific. The delayed oscillator mechanism thus embodies eastern Pacific air–sea interactions. The evolution of the 1997–98 El Niño, however, suggests that the western Pacific is also important for its development and decay.

Jin (1997) proposed a recharge–discharge oscillator model for ENSO that considers SST anomalies in the equatorial eastern Pacific and thermocline depth anomalies in the equatorial western Pacific. Westerly wind anomalies in the equatorial central Pacific deepens (raises) the equatorial thermocline in the east (west). The deepening of the thermocline in the east increases SST in the equatorial eastern Pacific bringing the system to a mature warm phase. At the same time, the divergence of zonally integrated Sverdrup transport causes heat to flow poleward from the equator. This discharge leads to a transition phase in which the entire equatorial Pacific thermocline is anomalously shallow. The anomalous shallow thermocline allows anomalous cold waters to be pumped into the surface layer by climatological upwelling and, therefore, decreases SST in the equatorial eastern Pacific and leads to a cold phase. The converse occurs during the cold phase of ENSO. Thus, the recharge and discharge of heat to the equator cause the coupled system to oscillate on an interannual timescale. Although Jin (1997) argued that the recharge–discharge oscillator model unlike the delayed oscillator is a basinwide oscillator, it does not consider off-equatorial western Pacific patterns. The 1997–98 El Niño shows that off-equatorial anomaly patterns and their associated equatorial wind anomalies in the western Pacific are important for its development and decay.

Based on the observations of Weisberg and Wang (1997b), Mayer and Weisberg (1998), and Wang et al. (1999) Weisberg and Wang (1997a) developed a western Pacific oscillator model for ENSO. This model considers the thermocline depth anomaly in the equatorial east-central Pacific, the equatorial zonal wind stress anomaly in the west-central Pacific, the off-equatorial thermocline depth anomaly in the western Pacific, and the equatorial zonal wind stress anomaly in the far western Pacific. Arguing from the vantage point of a Gill (1980) atmosphere, condensation heating due to convection in the equatorial west-central Pacific (Deser and Wallace 1990; Zebiak 1990) induces a pair of off-equatorial anomalous cyclones with westerly wind anomalies on the equator. These equatorial westerly wind anomalies deepen the thermocline and increase SST in the equatorial east-central Pacific, thereby providing a positive feedback for anomaly growth. Simultaneously, the off-equatorial anomalous cyclones raise the thermocline there via Ekman pumping. Thus, a shallow off-equatorial thermocline anomaly expands over the western Pacific leading to a decrease in SST and an increase in SLP in the off-equatorial western Pacific. During the mature phase of El Niño, the off-equatorial high SLP anomalies initiate equatorial easterly wind anomalies over the western Pacific. These equatorial easterly wind anomalies produce an upwelling/cooling oceanic response that proceeds eastward providing a negative feedback, while deepening the thermocline in the western Pacific.

Evolution of the 1997–98 El Niño from the onset phase to decay phase is consistent with the western Pacific oscillator. In the onset and development phases of the 1997–98 El Niño, twin off-equatorial anomalous cyclones are exhibited in the western Pacific. These off-equatorial anomalous cyclones produce equatorial westerly wind anomalies in the western Pacific. The equatorial westerly wind anomalies in the western Pacific cause the warming in the equatorial central and eastern Pacific. When the 1997–98 El Niño continues its growth, SST anomalies in the off-equatorial western Pacific reverse sign from warm to cold perhaps due to off-equatorial wind curl–induced Ekman pumping in the western Pacific. These off-equatorial cold SST anomalies are accompanied by the sign reversal of the off-equatorial SLP anomalies from low to high in the western Pacific. The off-equatorial high SLP anomalies initiates equatorial easterly wind anomalies over the western Pacific during the mature phase, which force eastward propagating Kelvin waves with upwelling tendency that provide a negative feedback for the coupled system. This negative feedback induced by local forcing in the western Pacific, along with the negative feedback by wave reflection at the western boundary, may help bring the 1997–98 El Niño toward its decay phase. As suggested by observations, more than one ENSO oscillator mechanisms may be at work.

Acknowledgments. This work was supported by the National Oceanic and Atmospheric Administration, Of-

fice of Global Programs, Grants NA66GPO119 and by the National Science Foudation, Division of Ocean Sciences, and by the NASA seasonal-to-interannual prediction project. We thank R. Reynolds at NOAA/NCEP for SST data, J. Janowiak at NOAA/NCEP for OLR data, M. Chelliah at NOAA/NCEP for NCEP–NCAR reanalysis SLP fields, and J. Stricherz and J. O'Brien at FSU for pseudostress data.

REFERENCES

Battisti, D. S., and A. C. Hirst, 1989: Interannual variability in the tropical atmosphere–ocean model: Influence of the basic state, ocean geometry and nonlinearity. *J. Atmos. Sci.,* **46,** 1687–1712.

Bell, G. D., and M. S. Halpert, 1998: Climate assessment for 1997. *Bull. Amer. Meteor. Soc.,* **79,** S1–S50.

Bjerknes, J., 1969: Atmospheric teleconnections from the equatorial Pacific. *Mon. Wea. Rev.,* **97,** 163–172.

Busalacchi, A., and J. J. O'Brien, 1981: Interannual variability of the equatorial Pacific in the 1960s. *J. Geophys. Res.,* **86,** 10 901–10 907.

Cane, M. A., M. Munnich, and S. E. Zebiak, 1990: A study of self-excited oscillations of the tropical ocean–atmosphere system. Part I: Linear analysis. *J. Atmos. Sci.,* **47,** 1562–1577.

Deser, C., and J. M. Wallace, 1990: Large-scale atmospheric circulation features of warm and cold episodes in the tropical Pacific. *J. Climate,* **3,** 1254–1281.

Gill, A. E., 1980: Some simple solutions for heat-induced tropical circulation. *Quart. J. Roy. Meteor. Soc.,* **106,** 447–462.

Jin, F. F., 1997: An equatorial ocean recharge paradigm for ENSO. Part I: Conceptual model. *J. Atmos. Sci.,* **54,** 811–829.

Kalnay, E., and Coauthors, 1996: The NCEP/NCAR 40-Year Reanalysis Project. *Bull. Amer. Meteor. Soc.,* **77,** 437–471.

Mayer, D. A., and R. H. Weisberg, 1998: El Niño–Southern Oscillation-related ocean–atmosphere coupling in the western equatorial Pacific. *J. Geophys. Res.,* **103,** 18 635–18 648.

McCreary, J. P., 1976: Eastern tropical ocean response to changing wind systems: With application to El Niño. *J. Phys. Oceanogr.,* **6,** 632–645.

——, and D. L. T. Anderson, 1991: An overview of coupled ocean–atmosphere models of El Niño and the Southern Oscillation. *J. Geophys. Res.,* **96,** 3125–3150.

McPhaden, M. J., 1999: Genesis and evolution of the 1997–98 El Niño. *Science,* **283,** 950–954.

Neelin, J. D., D. S. Battisti, A. C. Hirst, F.-F. Jin, Y. Wakata, T. Yamagata, and S. E. Zebiak, 1998: ENSO theory. *J. Geophys. Res.,* **103,** 14 262–14 290.

Philander, S. G., 1981: The response of equatorial oceans to a relaxation of the trade winds. *J. Phys. Oceanogr.,* **11,** 176–189.

——, 1985: El Niño and La Niña. *J. Atmos. Sci.,* **42,** 2652–2662.

——, 1990: *El Niño, La Niña, and the Southern Oscillation.* Academic Press, 289 pp.

Rasmusson, E. M., and T. H. Carpenter, 1982: Variations in tropical sea surface temperature and surface wind fields associated with the Southern Oscillation/El Niño. *Mon. Wea. Rev.,* **110,** 354–384.

Reynolds, R. W., and T. M. Smith, 1994: Improved global sea surface temperature analysis using optimum interpolation. *J. Climate,* **7,** 929–948.

——, and ——, 1995: A high-resolution global sea surface temperature climatology. *J. Climate,* **8,** 1571–1583.

Smith, T. M., R. W. Reynolds, R. E. Livezey, and D. C. Stokes, 1996: Reconstruction of historical sea surface temperature using empirical orthogonal functions. *J. Climate,* **9,** 1403–1420.

Stricherz, J., D. M. Legler, and J. J. O'Brien, 1997: *TOGA Pseudo-Stress Atlas 1985–94.* Vol. II, *Pacific Ocean,* The Florida State University, 155 pp.

Suarez, M. J., and P. S. Schopf, 1988: A delayed action oscillator for ENSO. *J. Atmos. Sci.,* **45,** 3283–3287.

Tang, T. Y., and R. H. Weisberg, 1984: On the equatorial Pacific response to the 1982/1983 El Niño–Southern Oscillation event. *J. Mar. Res.,* **42,** 809–829.

Wang, B., 1995: Interdecadal changes in El Niño onset in the last four decades. *J. Climate,* **8,** 267–285.

Wang, C., R. H. Weisberg, and J. I. Virmani, 1999: Western Pacific interannual variability associated with the El Niño-Southern Oscillation. *J. Geophys. Res.,* **104,** 5131–5149.

Weisberg, R. H., and C. Wang, 1997a: A western Pacific oscillator paradigm for the El Niño–Southern Oscillation. *Geophys. Res. Lett.,* **24,** 779–782.

——, and ——, 1997b: Slow variability in the equatorial west-central Pacific in relation to ENSO. *J. Climate,* **10,** 1998–2017.

Woodruff, S. D., R. J. Slutz, R. L. Jenne, and P. M. Steurer, 1987: A comprehensive ocean–atmosphere dataset. *Bull. Amer. Meteor. Soc.,* **68,** 1239–1250.

Wyrtki, K., 1975: El Niño—The dynamic response of the equatorial Pacific Ocean to atmospheric forcing. *J. Phys. Oceanogr.,* **5,** 572–584.

Yu, L., and M. M. Rienecker, 1998: Evidence of an extratropical atmospheric influence during the onset of the 1997–98 El Niño. *Geophys. Res. Lett.,* **25,** 3537–3540.

Zebiak, S. E., 1990: Diagnostic studies of Pacific surface winds. *J. Climate,* **3,** 1016–1031.